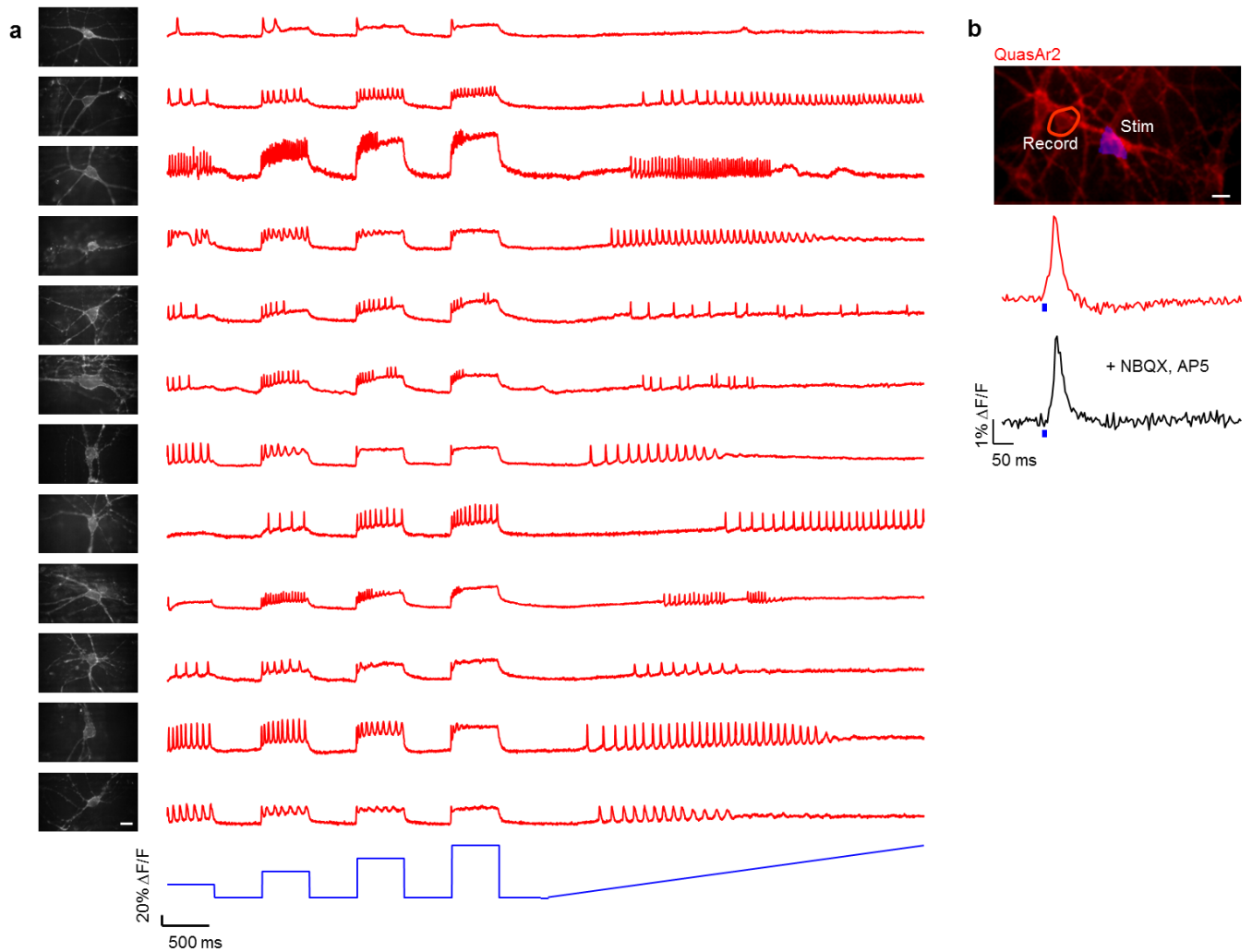


In the format provided by the authors and unedited.

All-optical synaptic electrophysiology probes mechanism of ketamine-induced disinhibition

Linlin Z. Fan ¹, Ralda Nehme^{2,3}, Yoav Adam¹, Eun Sun Jung⁴, Hao Wu ¹, Kevin Eggan^{2,3},
Don B. Arnold⁴ and Adam E. Cohen ^{1,5*}

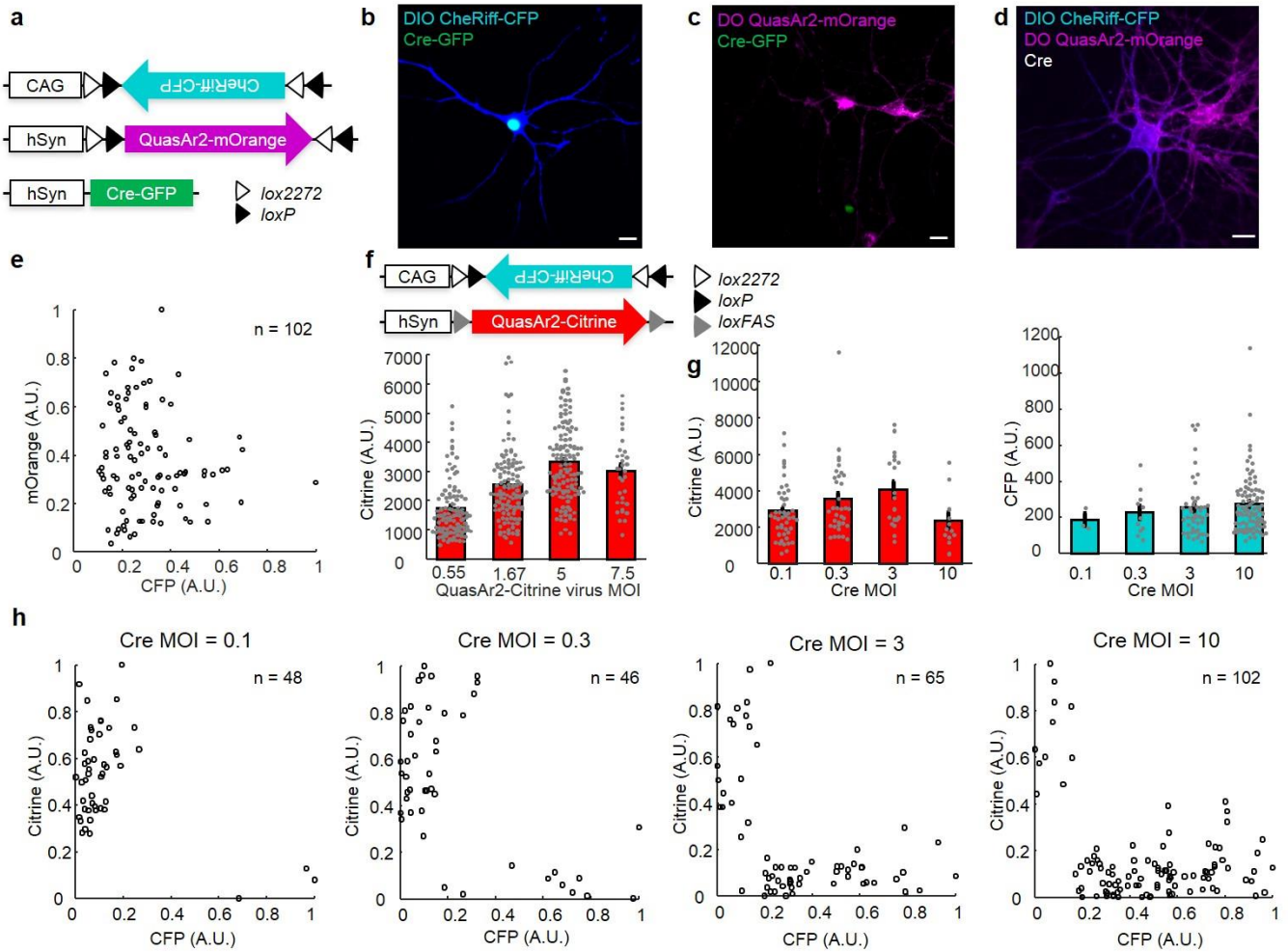
¹Department of Chemistry and Chemical Biology, Harvard University, Cambridge, MA, USA. ²Department of Stem Cell and Regenerative Biology, Harvard University, Cambridge, MA, USA. ³Stanley Center for Psychiatric Research, The Broad Institute of Harvard and MIT, Cambridge, MA, USA. ⁴Department of Biology, Section of Molecular and Computational Biology, University of Southern California, Los Angeles, CA, USA. ⁵Howard Hughes Medical Institute, Harvard University, Cambridge, MA, USA. *e-mail: cohen@chemistry.harvard.edu



Supplementary Figure 1

Co-expression of CheRiff- and QuasAr2-introduced optical crosstalk in measurements of synaptic transmission.

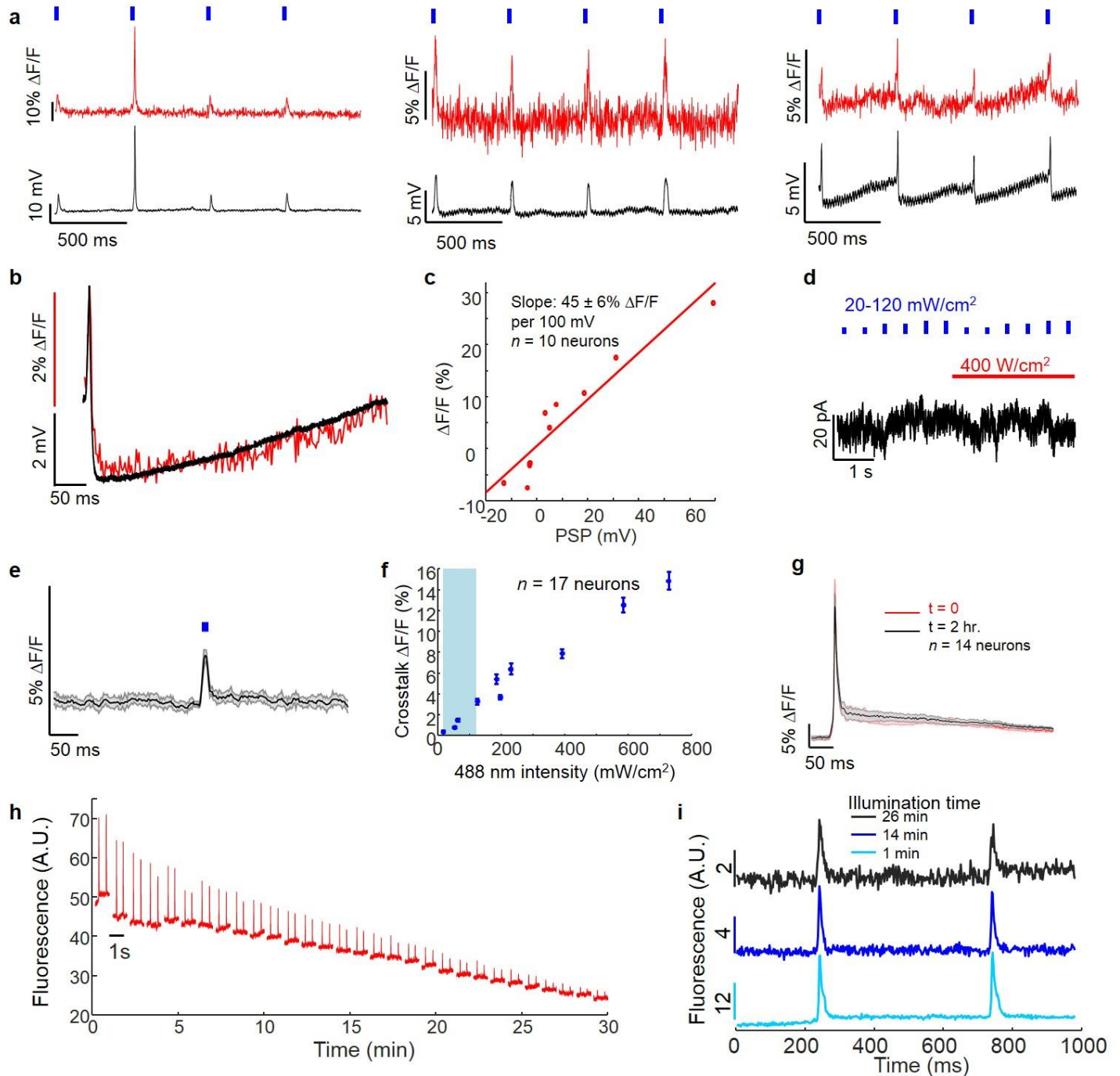
(a) In neurons co-expressing CheRiff-CFP and QuasAr2-Citrine, the QuasAr2 citrine fluorescence reported action potentials with high SNR. Left: Images of QuasAr2 fluorescence. Scale bar 20 μm . Right: fluorescence of QuasAr2 during optogenetic stimulation, recorded at 500 Hz. Blue: Optogenetic stimulation waveform. (b) Top: red: QuasAr2 fluorescence, blue: DMD mask for patterned blue light stimulation. Scale bar: 10 μm . Bottom: fluorescence signal of the circled cells before (red) and after (black) addition of excitatory blockers NBQX (20 μM) and AP5 (50 μM). The persistence of the signal indicates that it arose from direct optogenetic stimulation of a post-synaptic neurite rather than from synaptic transmission.



Supplementary Figure 2

Redundant use of Cre recombination sites caused spurious cross-reactivity.

(a) Schematic of DIO Cre-on CheRiff-CFP and DO Cre-off QuasAr2-mOrange. (b) Neurons co-infected with DIO Cre-on CheRiff-CFP and Cre-GFP showed Cre-activated expression. (c) Neurons co-infected with DO Cre-off QuasAr2-mOrange and Cre-GFP showed Cre-inactivated expression. (d) Neurons co-infected with DIO CheRiff-CFP, DO QuasAr2-mOrange and Cre did not show mutually exclusive expression of the actuator and reporter. Scale bars in (b)-(d) 20 μ m. (*n* in (b)-(d) = 3 culture dishes; representative data are shown) (e) Quantification of the data in (d) showing lack of mutually exclusive expression (*n* = 102 neurons). (f) Top: schematic of DIO Cre-on CheRiff-CFP and FAS Cre-off QuasAr2-Citrine. Bottom: mean expression levels of FAS Cre-off QuasAr2-Citrine depended on the titers of the FAS Cre-off QuasAr2-Citrine lentiviruses. (*n* = 391 neurons) (g) Mean expression levels in expressing cells of (left, *n* = 112 neurons) FAS Cre-off QuasAr2-Citrine and (right, *n* = 149 neurons) DIO Cre-on CheRiff-CFP did not depend on the titer of the Cre virus. (h) SynOptopatch constructs mediated mutually exclusive expression of actuator and reporter. No co-expression of DIO Cre-on CheRiff-CFP and FAS Cre-off QuasAr2-Citrine was observed across a range of titers of Cre virus. All statistics are mean \pm s.e.m. All error bars, s.e.m.

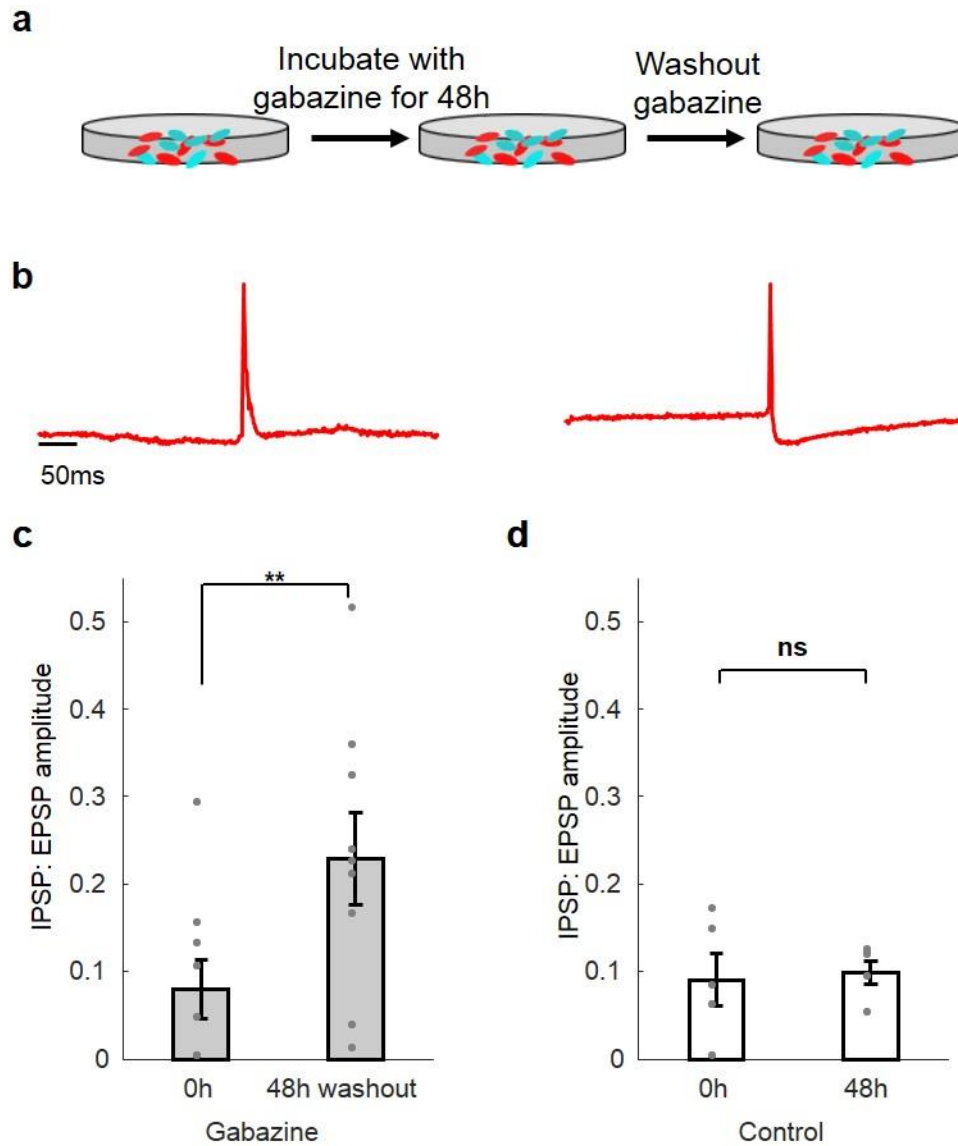


Supplementary Figure 3

Calibration of the synOptopatch constructs.

(a) Simultaneous fluorescence and manual patch clamp recordings of PSPs and APs evoked by presynaptic optogenetic stimulation. Blue, 10 ms blue light stimulation; red, whole-cell single-trial unfiltered fluorescence; black, patch-clamp recordings. (b) Overlay of mean optically and electrically recorded PSP waveforms from a single cell ($n = 9$ repeats). (c) Quantification of fluorescence vs. postsynaptic potential for synOptopatch recordings ($n = 10$ neurons, $R^2 = 0.9$). (d) Quantification of photocurrent of QuasAr2 under red and blue illumination (red: 400 W/cm^2 ; blue: 10 ms , $20 - 120 \text{ mW/cm}^2$). (e, f) Quantification of optical crosstalk of blue illumination into QuasAr2 fluorescence. (e) Neurons expressing QuasAr2 were exposed to continuous excitation at 640 nm and pulses of illumination at 488 nm (10 ms , 60 mW/cm^2) ($n = 17$ neurons). (f) Quantification of crosstalk amplitude as a function of blue light intensity. The shading represents the range of blue light intensity used for optogenetic stimulation of primary neurons. Error bars represent s.e.m. (g) SynOptopatch fluorescence recordings of EPSPs were stable for at least 2 h. (h) Photobleaching of QuasAr2 in the

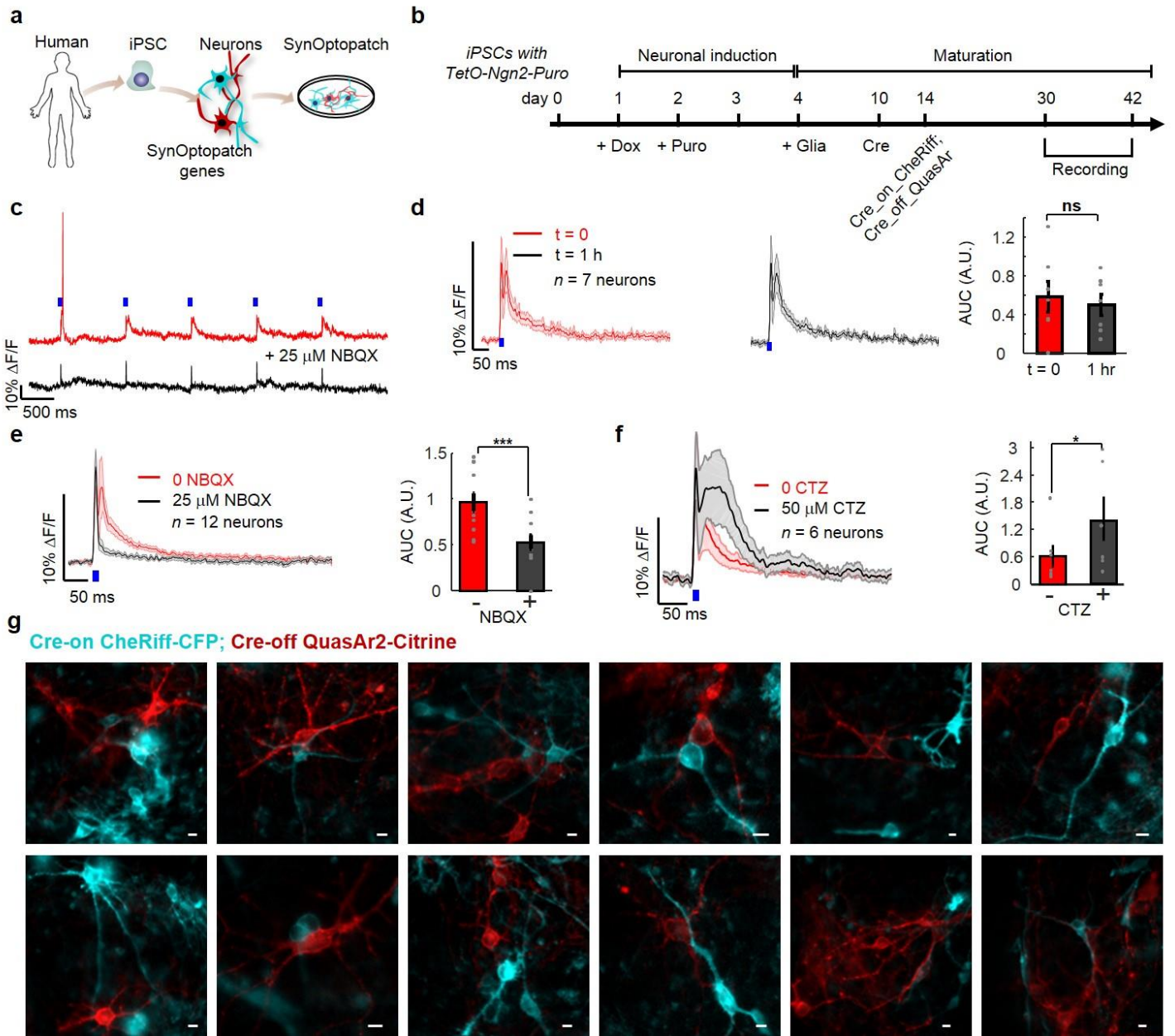
synOptopatch assay. A neuron was illuminated for 30 minutes continuously at 640 nm, 400 W/cm² and probed at 60 s intervals with blue light to induce PSPs (2 pulses of 10 ms, 2 Hz, 60 mW/cm²). (i) Stability of PSP waveform recorded as a function of duration of continuous red illumination. (In (h,i), $n = 3$ neurons; representative data are shown). All shaded error bars, s.e.m.



Supplementary Figure 4

SynOptopatch detects synaptic plasticity.

(a) Schematic showing protocol for inducing homeostatic plasticity. (b) A typical ten-trial average trace of a same neuron measured before gabazine incubation (left) and when wash-out after 48h incubation with gabazine (right). (c) Neurons incubated for 48h with gabazine had increased ratio of IPSP amplitude over EPSP amplitude ($n = 9$ neurons, $**p = 0.04$, two-sided paired-sample t-test), while (d) control cells did not show significant increase in the ratio of IPSP amplitude over EPSP amplitude ($n = 5$ neurons, $p = 0.76$, two-sided paired-sample t-test). All error bars, s.e.m. All statistics are mean \pm s.e.m.

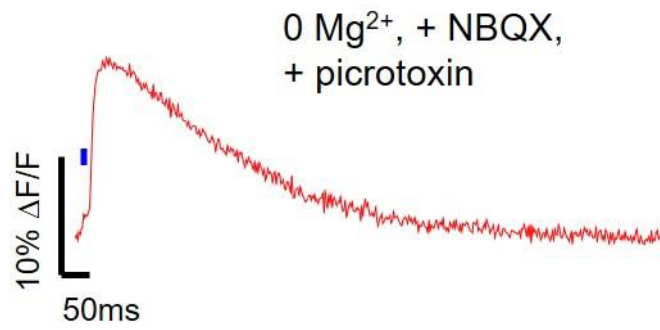


Supplementary Figure 5

SynOptopatch in hiPSC-derived neurons.

(a) Schematic of synOptopatch in hiPSC-derived neurons. (b) Schematic of excitatory cortical neuron differentiation, gene transduction, maturation and measurement. (c) Blue light stimulation induced single-trial PSPs and APs (red: before; black: after NBQX addition). Due to lower CheRiff expression than in primary neurons, stimulation required higher blue light intensities (400 mW/cm^2 vs. $20 - 120 \text{ mW/cm}^2$ for primary neurons) to evoke presynaptic APs. ($n = 12$ neurons; representative data are shown) (d) PSPs were stable for one hour (red: before; black: one hour without perturbation). Right: quantification of AUC before and after one hour (AUC, A.U., 0.58 ± 0.16 vs. 0.50 ± 0.11 , $n = 7$ neurons, $p = 0.4$, two-sided paired-sample t-test). (e) A synaptic blocker ($25 \mu\text{M}$ NBQX) largely eliminated the PSPs. The residual transient in the presence of NBQX occurred concurrent with the blue light stimulation, indicating that this signal arose from blue light crosstalk, a consequence of the higher blue stimulation power needed (also visible in (d) and (f)). Right: quantification of AUC before and after addition of NBQX (AUC, A.U., 0.97 ± 0.1 vs. 0.53 ± 0.07 , $n = 12$ neurons, $***p = 2 \times 10^{-5}$, two-sided paired-sample t-test). (f) A positive allosteric modulator of AMPARs and kainate receptors (cyclothiazide (CTZ), $50 \mu\text{M}$) increased the PSP amplitude. Right: quantification of AUC before and after addition of CTZ (AUC, A.U., 0.63 ± 0.26 vs. 1.4 ± 0.48 , $n = 6$ neurons, $*p = 0.055$, two-sided paired-sample t-test). (g) Exclusive expression of QuasAr2 and CheRiff in hiPSC derived neurons. Green:

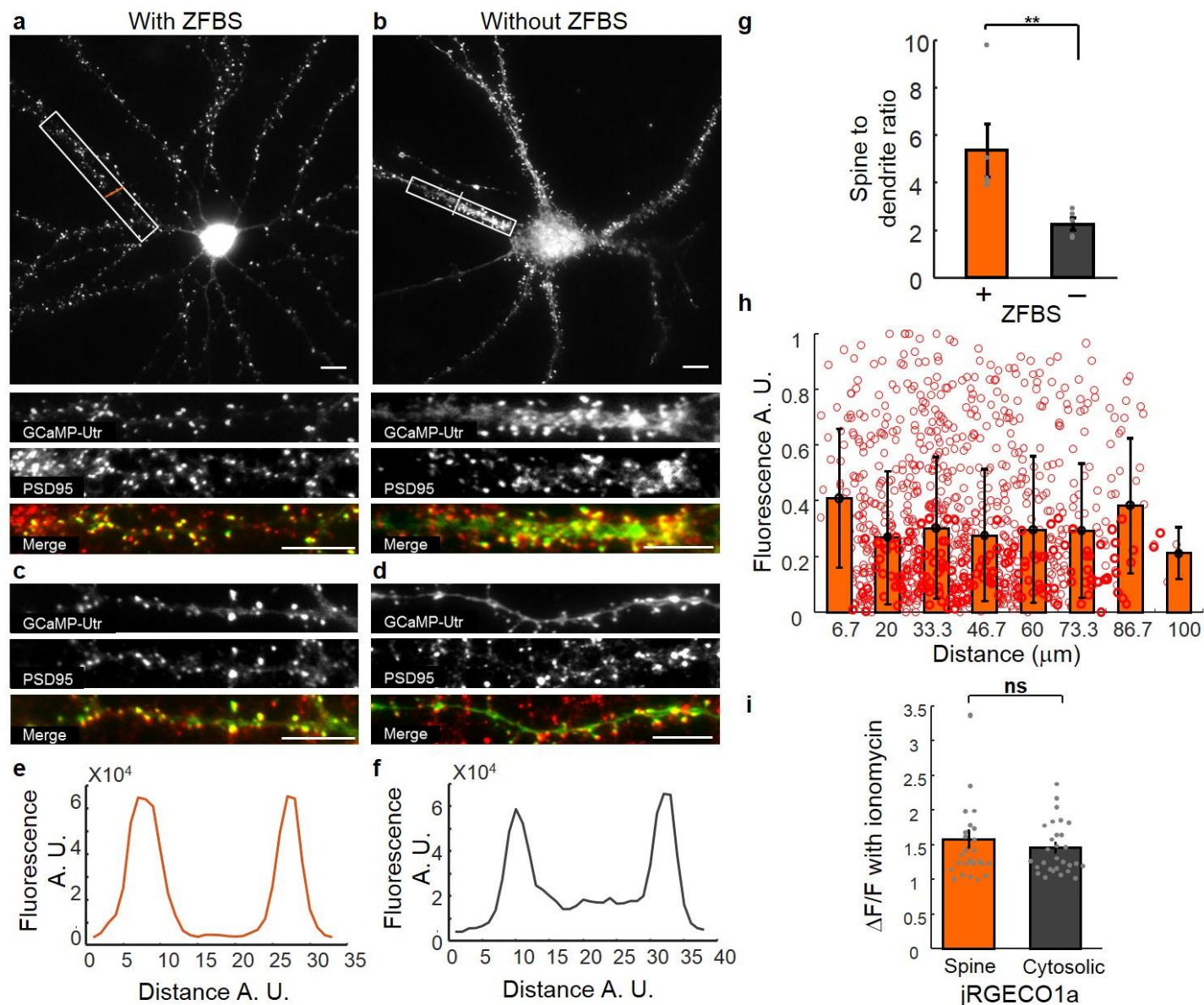
presynaptic cells expressing CheRiff-CFP. Red: postsynaptic cells expressing QuasAr2-Citrine, showing Citrine fluorescence. All scale bars 10 μm . ($n = 3$ culture dishes; representative data are shown) All shaded error bars and error bars, s.e.m. All statistics are mean \pm s.e.m.



Supplementary Figure 6

NMDAR component of postsynaptic potential.

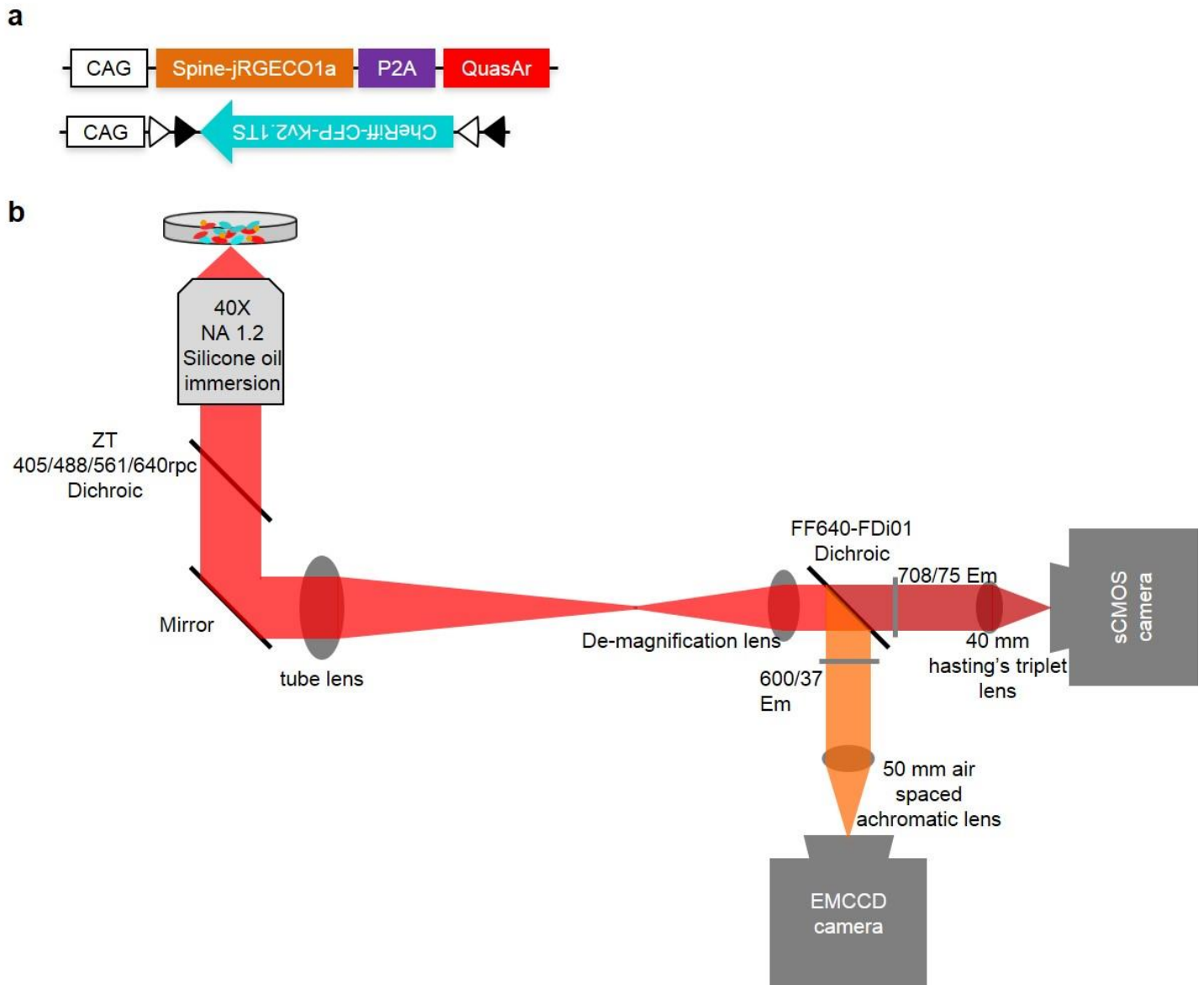
To isolate the NMDAR component of the PSP, we added 10 μM NBQX and 10 μM picrotoxin to block AMPA and GABA_A receptors, respectively, and imaged in a medium containing 0 Mg²⁺ to remove the voltage-dependent Mg²⁺ NMDAR block. Ten-trial average. ($n = 10$ neurons; representative data are shown)



Supplementary Figure 7

Targeting GCaMP6s and jRGECO1a to dendritic spines with and without transcriptional regulatory system.

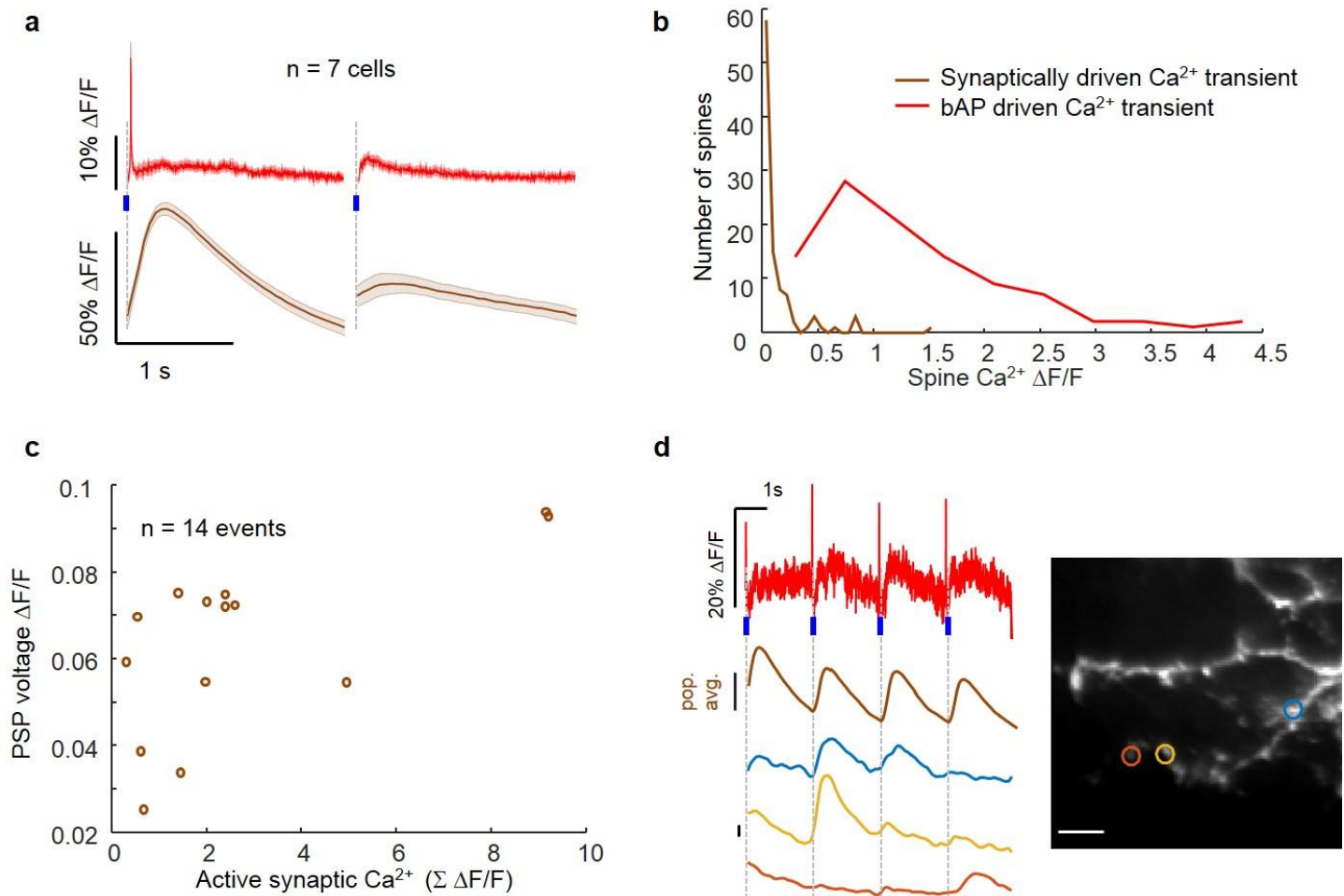
(a) Image of a neuron expressing GCaMP6s fused to the CH domain of Utrophin (GCaMP6s-Utr) with zinc finger binding sequence (ZFBS). GCaMP6s was stained with anti-GFP antibody. GCaMP6s co-localized with endogenous PSD-95, a marker for dendritic spines. PSD95 puncta not associated with GCaMP6s puncta were due to spines from neighboring neurons not expressing GCaMP6s. Scale bar: 10 μm. (b) GCaMP6s-Utr without ZFBS exhibited more diffuse localization compared to regulated GCaMP6s-Utr. (c,d) Examples from additional neurons as in a and b, respectively. (a-d, $n = 5$ neurons; representative data are shown) (e, f) Example fluorescence line sections transecting two spines and a parent dendrite along the lines shown in a and b, respectively. (g) Quantification of ratio of fluorescence in spines to adjacent parent dendrites in cells expressing GCaMP6-Utr with or without the ZFBS ($n = 5$ neurons of each type, ~200 spines/neuron, $**p = 0.027$, two-sided t-test). (h) Quantification of spine fluorescence as a function of distance from the soma ($n = 5$ neurons of each type, ~200 spines/neuron). (i) Spine-jRGECO1a and cytosolic jRGECO1a expressed in HEK293 cells gave the same fluorescence response to a Ca^{2+} transient induced by 10 μM ionomycin ($\Delta F/F$ 1.6 ± 0.1 vs. 1.5 ± 0.07 , $n = 26$ cells for spine-jRGECO1a, $n = 29$ for cytosolic jRGECO1a, $p = 0.4$, two-sided student's t-test). All error bars, s.e.m. All statistics are mean \pm s.e.m.



Supplementary Figure 8

Simultaneous imaging of spine-jRGECO1a and QuasAr2.

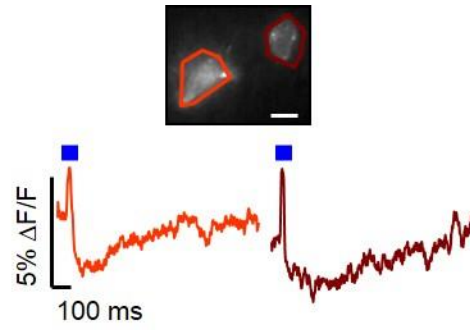
(a) Co-expression of spine-jRGECO1a and QuasAr2. Schematic showing three color imaging with blue light excitable soma-localized CheRiff in presynaptic cells, yellow light excitable spine-jRGECO1a and red light excitable QuasAr2 co-expressed in postsynaptic cells. (b) Dual-view microscope for simultaneous imaging of spine-jRGECO1a and QuasAr2. Fluorescence from spine-jRGECO1a and QuasAr2 were passed to EMCCD camera and sCMOS camera, respectively, by a 640 nm dichroic beamsplitter.



Supplementary Figure 9

Correlation of synaptic and bAP induced Ca²⁺ activity in dendritic spines.

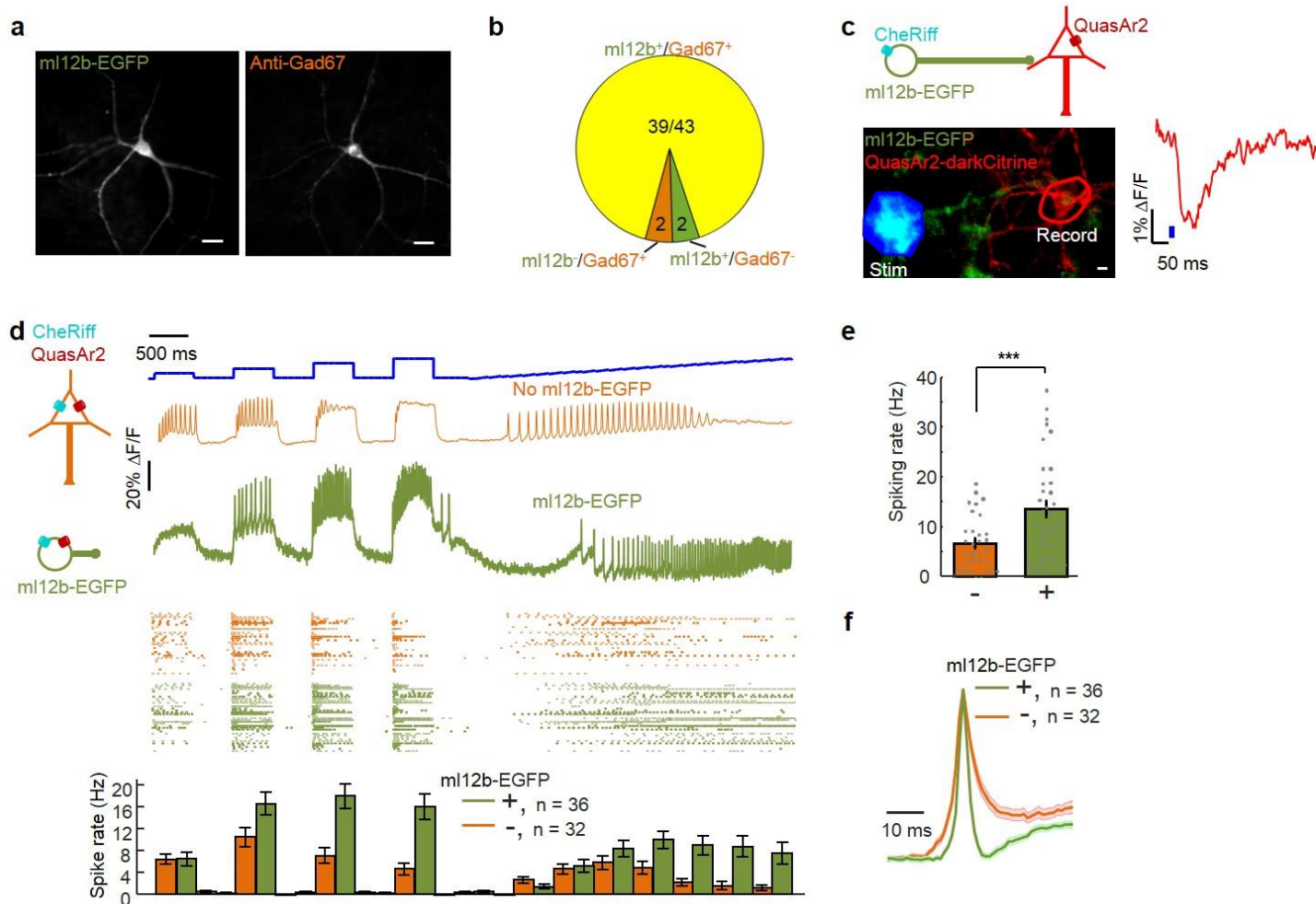
(a) Red: mean AP and PSP reported by QuasAr2; orange: mean spine-jRGECO1a fluorescence induced by bAP and sub-threshold synaptic inputs, respectively. (b) Distribution of Ca²⁺ transient amplitudes in spines, induced by bAPs (red) or subthreshold synaptic inputs (brown). Synaptic inputs only drove Ca²⁺ transients in a subset of synaptic spines, while bAPs drove Ca²⁺ signals synchronously in almost all dendritic spines. (c) Correlation of somatic PSPs and sum of Ca²⁺ transient amplitude across all spines ($n = 14$, $R^2 = 0.42$, $p = 0.01$). (d) bAP failure in spines. Blue: 10 ms blue light stimulation of soma-localized ChR2 in a presynaptic cell. Red: Postsynaptic QuasAr2 fluorescence; dark yellow: average over all the spines of spine-jRGECO1a fluorescence ($n = 100$ spines). Right: Single-spine fluorescence traces within a single dendritic branch, corresponding to the regions circled in the figure. The orange trace shows an example of a bAP-induced spine Ca²⁺ transient distal to a spine which did not respond to the bAP. Scale bar 15 μ m. All shaded error bars, s.e.m.



Supplementary Figure 10

IPSPs in acute slices under high K^+ concentration.

IPSP detected under the condition of 5 mM K^+ , twice higher than usual ACSF, and 10 μ M NBQX, 10 μ M AP5. Blue: 10 ms blue light stimulation. Light and dark red: IPSPs. Scale bar 10 μ m. Five-trial average. ($n = 8$ cells; representative data are shown).



Supplementary Figure 11

Development and characterization of an inhibitory neuron-specific enhancer.

(a) The inhibitory marker Gad67 co-localized with eGFP expression. Left: mI12b-eGFP; Right: anti-GAD67 immunostaining (*Methods*). Scale bars: 30 μm . ($n = 39$ cells; representative data are shown). (b) Correspondence of mI12b-eGFP fluorescence and Gad67 immunostaining in neurons that were positive for at least one of these reporters. Of $n = 41$ Gad67⁺ neurons, 39 were mI12b-eGFP⁺. Of $n = 41$ mI12b-eGFP⁺ neurons, 39 were also Gad67⁺. (c) Top: Schematic showing patterned light stimulation onto an mI12b-eGFP⁺ neuron and voltage imaging from a nearby cell expressing QuasAr2. Middle: dark green: mI12b-eGFP, red: QuasAr2-dark Citrine, blue: DMD mask for patterned blue light stimulation. Right: IPSP was evoked by stimulation of the presynaptic cell expressing mI12b-EGFP. Scale bar: 10 μm . Two-trial average. ($n = 3$ cells; representative data are shown). (d) Optopatch measurements of spiking patterns and AP waveforms revealed differences between mI12b-eGFP⁺ and mI12b-eGFP⁻ neurons consistent with differences between inhibitory vs. excitatory neurons reported by patch clamp measurements (*Methods*).^{36 37} Blue: blue light stimulation of cells expressing both CheRiff and QuasAr2. Example traces show QuasAr2 fluorescence from a nominal excitatory neuron (orange, mI12b-EGFP⁻) and a nominal inhibitory neuron (green, mI12b-EGFP⁺). Middle: raster plots of spiking. Bottom: spike rate of nominal excitatory neurons (orange, mI12b-EGFP⁻) and inhibitory neurons (green, mI12b-EGFP⁺). (e) Spiking rate and (f) spiking waveform of cells not expressing mI12b (orange) and expressing mI12b (dark green). All shaded error bars and error bars, s.e.m. mI12b-eGFP⁺ neurons (putative interneurons) showed higher average evoked firing rates (13.6 ± 1.7 vs. 6.7 ± 1 Hz, $p = 0.001$, two-sided two-sample t-test), lower probability of depolarization block under strong stimulus, narrower action potentials (6.9 ± 0.2 ms vs. 9.4 ± 0.4 ms, $p = 1 \times 10^{-6}$, two-sided two-sample t-test) and larger after-hyperpolarization compared to simultaneously measured mI12b-eGFP⁺ cells ($n = 36$ mI12b-eGFP⁺ and 32 mI12b-eGFP⁻ neurons).

Supplementary Tables

| Table S1 synOptopatch constructs | Vector | Addgene |
|---|---------------|----------------|
| LZF40: hSyn-Cre | Lenti-vector | 109378 |
| LZF43: Cre-on CAG-CheRiff-CFP (DIO) | Lenti-vector | 104114 |
| LZF80: Cre-on CAG-CheRiff-soma-CFP (DIO) | Lenti-vector | 104115 |
| LZF42: Cre-off hSyn-QuasAr2-Citrine (<i>FAS</i>) | Lenti-vector | 104116 |
| LZF70: Cre-off hSyn-QuasAr2-dark Citrine (<i>FAS</i>) | Lenti-vector | 104117 |
| LZF39: Cre-off hSyn-CheRiff-CFP (<i>FAS</i>) | Lenti-vector | 104118 |
| LZF1718: Cre-off hSyn-CheRiff-CFP (<i>FAS</i>) | AAV vector | 104119 |
| LZF94: Cre-on CAG-spine-GCaMP6s | AAV vector | 104120 |
| LZF97: hSyn-spine-jRGECO1a | Lenti-vector | 104121 |
| LZF1604: CAG-spine-jRGECO1a-P2A-QuasAr2-dark Citrine | pcDNA | 104122 |
| LZF1723: mI12b-EGFP | Lenti-vector | 104123 |